

 Open access • Journal Article • DOI:10.1007/S00226-017-0936-3

## Dielectric and mechanical properties of various species of Madagascan woods

— [Source link](#) 

Frédéric Roig, Georgette Ramanantsizehena, Fils Lahatra Razafindramisa, Eric Dantras ...+4 more authors

**Institutions:** University of Toulouse, University of Antananarivo

**Published on:** 29 Jun 2017 - Wood Science and Technology (Springer Berlin Heidelberg)

Related papers:

- [Investigation of the effect of aging on wood hygroscopicity by 2D 1H NMR relaxometry](#)
- [Solid-State Nmr Studies Of Wood And Other Lignocellulosic Materials](#)
- [FTIR analysis of chemical changes in wood induced by steaming and longitudinal compression](#)

Share this paper:    

View more about this paper here: <https://typeset.io/papers/dielectric-and-mechanical-properties-of-various-species-of-3g8r9lhn3m>



## Open Archive TOULOUSE Archive Ouverte (OATAO)

OATAO is an open access repository that collects the work of Toulouse researchers and makes it freely available over the web where possible.

This is an author-deposited version published in : <http://oatao.univ-toulouse.fr/>  
Eprints ID : 19428

**To link to this article** : DOI : 10.1007/s00226-017-0936-3  
URL : <http://dx.doi.org/10.1007/s00226-017-0936-3>

**To cite this version** : Roig, Frédéric and Ramanantsizehena, Georgette and Lahatra Razafindramisa, Fils and Dantras, Eric and Dandurand, Jany and Hoyet, Hervé and Bernes, Alain and Lacabanne, Colette *Dielectric and mechanical properties of various species of Madagascan woods*. (2017) Wood Science and Technology, vol. 51 (n° 6). pp. 1389-1404. ISSN 0043-7719

Any correspondence concerning this service should be sent to the repository administrator: [staff-oatao@listes-diff.inp-toulouse.fr](mailto:staff-oatao@listes-diff.inp-toulouse.fr)

## Dielectric and mechanical properties of various species of Madagascan woods

Frédéric Roig<sup>1</sup> · Georgette Ramanantsizehena<sup>2</sup> ·  
Fils Lahatra Razafindramisa<sup>2</sup> · Eric Dantras<sup>1</sup> ·  
Jany Dandurand<sup>1</sup> · Hervé Hoyet<sup>1</sup> · Alain Bernés<sup>1</sup> ·  
Colette Lacabanne<sup>1</sup>

**Abstract** The low-temperature molecular mobility of three different wood species was analyzed, with the two major constituents—cellulose and lignin—as reference. Mechanical and dielectric dynamic techniques were used. In order to observe the fine structure of the broad relaxation modes of wood, a very low-frequency analysis was carried out by thermostimulated current technique. Low-temperature relaxations of rosewood were assigned to low-temperature relaxations of cellulose. There was no dielectric response of lignin in rosewood. Contrarily, both cellulose and lignin responses were distinguished in ebony and varongy. Thermostimulated currents analyses exhibit the specific behavior of lignin in the various wood species. Moreover, the relaxation mode of cellulose observed at lower temperature remains localized in rosewood, while it tends to delocalize in varongy and ebony. The nature and intensity of physical interactions that induce variation of phase miscibility might be responsible for the observed differences. Even at the scale of the  $\gamma$  relaxation, physical interactions modify molecular mobility.

### Introduction

Dynamic dielectric and mechanical properties of wood are widely investigated in the literature. Both are governed by molecular mobility, but their assignment to precise entities is still a subject of controversy. Maeda and Fukada (1987) investigated the effect of bound water on piezoelectric, dielectric and elastic

---

✉ Eric Dantras  
eric.dantras@univ-tlse3.fr

<sup>1</sup> CIRIMAT, Université de Toulouse, Physique des Polymères, 118 route de Narbonne, 31062 Toulouse, France

<sup>2</sup> Faculté des Sciences, Université d'Antananarivo, Antananarivo, Madagascar

---

properties of two materials of lignocellulosic composition: bamboo and cedar. Hirai et al. (1992) investigated piezoelectric relaxations of wood in the high temperature range. Two years later, Badry et al. (1994) compared dielectric permittivity of wood pulp with cotton linters and lignin. They highlighted the temperature influence on the dielectric permittivity. Duchow and Gerhardt (1996) reported on a dielectric characterization of wood and wood infiltrated with ceramic precursor. Hoffmann and Poliszko (1996) established temperature–frequency dependence by dielectric thermal analysis of wood. Mechanical and dielectric relaxations of wood were studied in the low temperature range by Obataya et al. (1996). Kabir et al. (1997) investigated the influence of hydration on dielectric properties of wood at room temperature and at different frequencies. They also studied ultrasonic properties of rubber wood as a function of moisture content, grain direction and frequency (Kabir et al. 1998a, b; Khalid et al. 1999). Mobarak et al. (1999) and Mounier et al. (1999) explored the electrical properties of agricultural residue papers. Kabir et al. (2000) established an equivalent circuit modeling of the dielectric properties of rubber wood at low frequency. Dielectric and electromagnetic properties were compared by Makoviny (2000). Yokoyama et al. (2000a, b) studied mechanical and dielectric relaxations of wood in the low temperature range. The number of adsorbed water molecules was estimated at various relative humidities by a model of elemental cell wall (Yokoyama 2000a, b). Backman and Lindberg (2001) were interested in differences in radial and tangential direction of wood material as observed by dynamic mechanical thermal analysis. Cao and Zhao (2001) and Obataya et al. (2001) analyzed the molecular mobility of absorbed water molecules in wood using dielectric analyses. Nakano (2004) prepared a review on mechanical relaxation and physical properties of wood. Sahin and Ay (2004) studied dielectric properties of hardwood at microwave frequencies and determined a general behavior. The grain direction of the wood plays an important role (Sahin and Ay 2004). Daian et al. (2005) established a method for measuring dielectric properties at microwave frequencies. Nakano (2005) studied the effect of quench on relaxation properties of wet wood. Sugimoto and Norimoto (2005) and Sugimoto et al. (2005) analyzed dielectric relaxation of charcoal wood and wood with high moisture content in the temperature range from  $-150$  to  $20$  °C and frequency range from  $20$  Hz to  $10$  MHz. Daian et al. (2006) made a model of the dielectric properties of wood. The influence of volume humidity on the dielectric properties of different wood species was studied by Romanov (2006). Jafarpour et al. (2008) observed in poplar wood, at low temperature, dielectric relaxation modes that were assigned to the molecular mobility of lignin and cellulose. Koubaa et al. (2008) measured the dielectric properties of four Canadian wood species using the cavity perturbation technique. After studies on charcoal and moist wood, Sugimoto et al. (2008a) analyzed the dielectric relaxation of water adsorbed on cellulose. The same group investigated the effect of various organic solvents on rheological properties of wood (Sugimoto et al. 2008b). Wang et al. (2008) analyzed the effect of lignin on wood matrix and examined the dielectric properties of untreated and delignified wood before and after quenching from  $50$  Hz to  $100$  MHz at  $20$  °C. Dielectric properties were widely used to explore the influence of various parameters and in particular moisture content on a series of materials of lignocellulosic composition (Tomppo et al. 2009;

---

Ramasamy and Moghtaderi 2010; Chilcott et al. 2011; Agoudjil et al. 2011). Recently, bionanocomposites based on poly (D, L-lactide) and cellulose nanowhiskers were investigated (Luiz de Paula et al. 2011); a review by Jonoobi et al. 2015 shows the variety of nanostructured cellulose extracted from various natural resources and bioreinforced nanocomposites (Marianoa et al. 2016).

This literature survey demonstrated that dielectric techniques are well suited to identify specific entities in wood polymers. The specificity of this study is to establish links between species and the arrangement of the various macromolecules in wood. Indeed, wood always constitutes cellulose microfibrils, hemicelluloses and lignin, but composition and molecular packing vary from one species to another. The macromolecular arrangement stabilized by physical interactions is characterized by molecular dynamics responsible for anelastic and dielectric properties. A thorough analysis of such dynamic behaviors might allow to shed some light on the macromolecular intrication of the constituting macromolecules in wood. Three wood species from Madagascar, ebony (*Diospyros sp.*), rosewood (*Dalbergia maritima sp.*) and varongy (*Ocotea sp.*) were analyzed in this study. Moreover, the authors worked at constant hydration level in order to concentrate on molecular mobility of the polymeric components of the different species.

## Materials and methods

### Materials

Cellulose and lignin were provided by Sigma-Aldrich. The cellulose is a white microcrystalline powder (20  $\mu\text{m}$ ) extracted from cotton linters, with a number-average molecular weight between 36000 and 40000. The degree of polymerization is between 222 and 246. The lignin is a brown powder extracted from sugar cane. All powder samples (cellulose and lignin) were pressed at controlled pressure of about 75 MPa to form pellets. Wood samples provided by the University of Antananarivo (Madagascar) are the three species: ebony, varongy and rosewood. All wood samples were extracted from sapwood. Sapwood of ebony is white. Its thickness varies between 4 and 8 cm. Sapwood of varongy is of light color with a thickness from 4 to 5 cm. Sapwood of rosewood is also of light color with a thickness between 4 and 6 cm. For each species, samples extracted from two different trees were studied, and the reproducibility was checked over three samples.

### Methods

#### *Thermostimulated currents (TSC)*

TSC measurements were taken with a homemade equipment previously described (Teyssedre and Lacabanne 1995). Samples (square of 15 mm by 15 mm; 0.5 mm thick) were inserted between two steel plate electrodes. The reproducibility was checked over six samples. Sample cell was filled with dry helium. For recording of complex thermograms, the sample was polarized by an electrostatic field  $E_p = 1 \text{ MV/m}$  during

$t_p = 2$  min over a temperature range from the polarization temperature  $T_p$  down to the freezing temperature  $T_0$ . Then, the field was turned off and the depolarization current was recorded with a constant heating rate ( $q_h = +7$  °C.min<sup>-1</sup>): The equivalent frequency of the TSC spectrum was  $f_{eq} \sim 10^{-2}$ – $10^{-3}$  Hz. Complex thermograms are generally due to multiple processes. In order to isolate each elementary process, complex thermograms are experimentally decomposed into elementary thermograms.

Elementary TSC thermograms were obtained with a poling window of 5 °C. Then, the field was removed and the sample cooled down to a temperature  $T_{cc} = T_p - 40$  °C. The depolarization current was normalized to be homogeneous with dipolar conductivity  $\sigma$ , and it was recorded with a constant heating rate  $q_h$ . The series of elementary thermograms was recorded by shifting the poling window by 5 °C toward higher temperature (Teyssedre and Lacabanne 1995). In this procedure, each elementary thermogram can be considered as a Debye process characterized by a single relaxation time  $\tau(T)$ . The temperature dependence of the dielectric relaxation time can be determined by Eq. 1 (Jafarpour et al. 2008):

$$\tau(T) = \frac{1}{q \times I(T)} \cdot \int_T^{T_f} I(T) \cdot dT, \quad (1)$$

where  $q$  is the heating rate and  $I(T)$  is the temperature-dependant depolarization current.

In the materials studied, the relaxation time  $\tau(T)$  of all elementary spectra versus  $1/T$  is linear and obeys the Arrhenius–Eyring equation (Eq. 2) (Jafarpour et al. 2008):

$$\tau(T) = \frac{h}{k_B T} \exp\left[-\frac{\Delta S}{R}\right] \exp\left(\frac{\Delta H}{RT}\right) = \tau_0 \exp\left[\frac{\Delta H}{RT}\right], \quad (2)$$

where  $R$  is the ideal gas constant,  $k_B$  is the Boltzmann constant,  $h$  is the Planck constant,  $\Delta H$  is the activation enthalpy,  $\Delta S$  is the activation entropy, and  $\tau_0$  is the pre-exponential factor.

According to the analysis of Starkweather (1981, 1990) and Starkweather and Avakian (1989), the activation enthalpy is due to two contributions: theoretical enthalpy related to the  $\Delta S = 0$  and the entropic enthalpy  $\Delta S \neq 0$ . The following relationship is proposed from Arrhenius equation (Jafarpour et al. 2008):

$$\Delta H = \Delta H^\ddagger (\Delta S = 0) + T \Delta S^\ddagger. \quad (3)$$

For relaxations having no activation entropy, Eq. 3 is reduced to the following relationship (Jafarpour et al. 2008):

$$\Delta H = \Delta H^\ddagger = RT \left[ 1 + \ln\left(\frac{k_B \cdot T}{2\pi h \cdot f_{eq}}\right) \right], \quad (4)$$

where  $f_{eq}$  is the equivalent frequency of electrical sollicitation of TSC  $\cong 10^{-3}$  Hz.

According to the hypothesis by Hoffman et al. (1966), activation entropy  $\Delta S$  and activation enthalpy  $\Delta H$  are linked with the size of mobile entity (Hoffman et al. 1966; Crine 1984, 2005; Yelon et al. 1992).

---

### *Dynamic dielectric spectroscopy (DDS)*

A BDS 4000 Novocontrol broadband dielectric spectrometer system was used to obtain the dielectric relaxation map in a wide temperature and frequency range. Samples (square of 15 mm by 15 mm; 0.5 mm thick) were inserted between two parallel electrodes. The reproducibility was checked over six samples. A sinusoidal electrical field was applied at a given temperature, and the complex impedance was recorded during a frequency scan. The measurements were taken in the frequency range (F)  $10^{-1}$ – $10^6$  Hz from  $-150$  to  $200$  °C by steps of  $5$  °C. The complex dielectric permittivity  $\varepsilon^*(\omega)$  was deduced from the complex impedance  $Z^*$  by Eq. 5 (Jafarpour et al. 2008):

$$\varepsilon^*(\omega) = \frac{1}{i\omega \cdot C_0 Z^*(\omega)} = \varepsilon' - i\varepsilon'' \quad (5)$$

with  $C_0$  the capacitance in vacuum and  $\omega$  the angular frequency ( $\omega = 2\pi F$ ). Relaxation modes are described by Havriliak–Negami (HN) function (Havriliak and Negami 1966) giving Eq. 6:

$$\varepsilon^*(\omega) = \varepsilon_\infty + \frac{\Delta\varepsilon}{[1 + (i\omega\tau_{HN})^{\alpha_{HN}}]^{\beta_{HN}}}, \quad (6)$$

where  $\tau_{HN}$  is the average relaxation time of the HN equation,  $\alpha_{HN}$  is the width, and  $\beta_{HN}$  is the asymmetry of the mode.

For comparative studies, the normalized loss permittivity, i.e., the loss tangent  $\tan\delta = \varepsilon''/\varepsilon'$ , was used. The shift of the maximum temperature  $T$  is recorded as a function of the angular frequency  $\omega$  or the average relaxation time  $\tau$ :  $\omega\tau = 1$ . Then, the Arrhenius diagram  $\ln\tau$  versus  $T^{-1}$  gives the activation enthalpy of the relaxation mode.

### *Dynamic mechanical analysis (DMA)*

Dynamic mechanical analyses were performed using a strain-controlled dynamic rheometer (ARES TA Instruments) in the torsion rectangular mode. This mode was more convenient for studying rigid samples in the linear range. Typical dimensions of specimens were  $40 \times 13 \times 0.5$  mm<sup>3</sup>. The reproducibility was checked over six samples. This apparatus was able to register the complex shear modulus  $G^* = G' + iG''$  under precise control of temperature. The component  $G'$ , called “storage modulus,” represents the conservative behavior, whereas the loss modulus  $G''$  relates to the dissipative energy. Often, the normalized loss modulus, i.e., loss tangent  $\tan\delta = G''/G'$ , is used for comparative studies. The thermomechanical measurements were taken at a heating rate of  $3$  °C/min from  $-150$  to  $200$  °C and at a constant oscillating angular frequency ( $\omega = 1$  rad/s).

---

## Results and discussion

### Extracted cell wall polymers

Cellulose and lignin were studied by DDS in the low temperature range where the signals characteristic of molecular mobility are observed (Jafarpour et al. 2008). The dielectric loss factor  $\tan(\delta)$  at the frequency of 1 Hz is presented in Fig. 1. At this frequency, these two polymers present a broad relaxation between  $-160$  and  $-20$  °C. The cellulose relaxation has its maximum around  $-120$  °C and the lignin relaxation around  $-80$  °C. These two relaxations are analyzed as a function of frequency, and the shift of the maximum is plotted in an Arrhenius diagram (inset in Fig. 1). The overall behavior of these two relaxations is similar, and their average relaxation times follow an Arrhenius equation. The activation enthalpy of cellulose/lignin is 46/49 kJ/mol, i.e., of the same order of magnitude. Contrarily, activation entropy for cellulose is  $72 \text{ J mol}^{-1} \text{ K}^{-1}$ , the double of the one of lignin. Consequently, according to these results the molecular mobility of cellulose in the low temperature range is more delocalized than the one of lignin. Moreover, TSC analysis will allow to explore the fine structure of the low-temperature mode of cellulose.

TSC analyses reveal the complexity of the relaxation observed in cellulose. The normalized depolarization current  $\sigma$  versus temperature is reported in Fig. 2. In this figure, the complex thermogram plotted from  $-160$  to  $-20$  °C highlights two relaxation modes:  $\gamma$  and  $\beta$ . The  $\gamma$  relaxation mode is characterized by an intense and broad peak with a maximum at  $-135$  °C. The  $\beta$  relaxation mode appears as a shoulder with a maximum at  $-65$  °C. These two relaxation modes have been resolved experimentally in a series of elementary thermograms revealing the existence of a discrete distribution of relaxation times. According to the literature, the  $\gamma$  relaxation mode of cellulose has been attributed to molecular mobility of

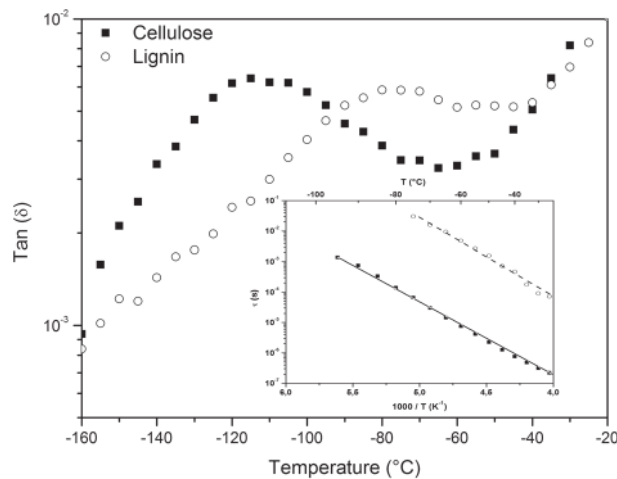


**Fig. 1** Dielectric  $\tan\delta$  versus temperature at the frequency  $F = 1$  Hz of the low-temperature relaxation mode observed by DDS for cellulose (*black square*) and lignin (*open circle*); *inset* Arrhenius diagram of the average relaxation time from  $10^{-1}$  to  $10^{+6}$  isofrequencies



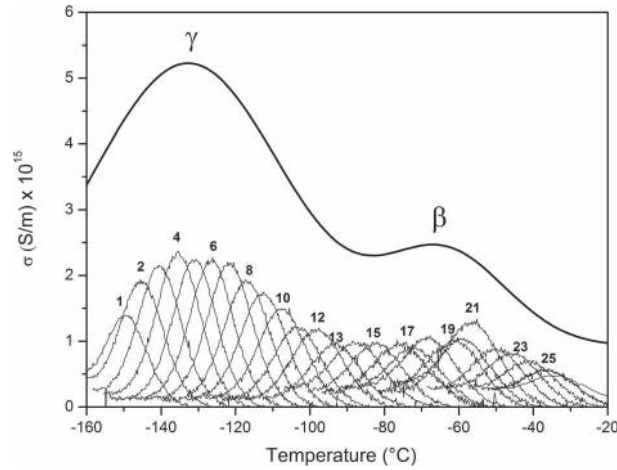


**Fig. 2** Complex TSC thermogram of cellulose superimposed with its fine structure (elementary TSC thermograms) obtained by using fractional polarizations

lateral groups of glycosidic rings ( $-\text{OH}$  and  $-\text{CH}_2\text{OH}$ ) (Saad et al. 1996; Saad and Furuhashi 1997; Einfeldt et al. 2000a, b, 2001, 2003; Einfeldt and Kwasniewski 2002; Meissner et al. 2000; Jafarpour et al. 2007, 2009; Roig et al. 2011a) and the  $\beta$  relaxation mode of cellulose to molecular mobility of glycosidic rings thanks to  $\beta_{1-4}$  glycosidic bonds (Saad et al. 1996; Saad and Furuhashi 1997; Einfeldt et al. 2000a, b, 2001, 2003, 2004; Einfeldt and Kwasniewski 2002; Meissner et al. 2000; Jafarpour et al. 2007, 2009). Lignin has also been studied by TSC in the low temperature range. The normalized depolarization current  $\sigma$  versus temperature is plotted in Fig. 3. The complex thermogram plotted from  $-140$  to  $-50$  °C highlights

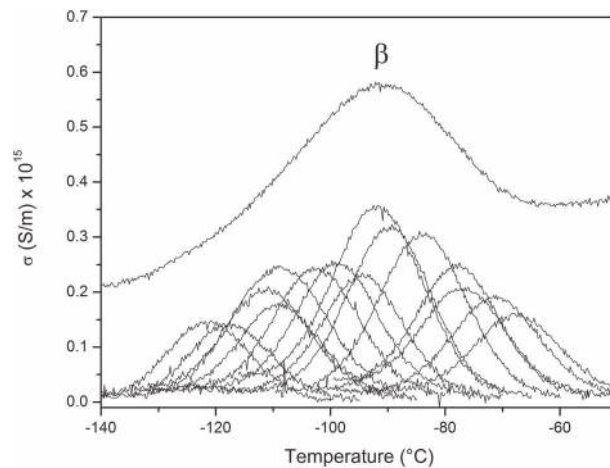


**Fig. 3** Complex TSC thermogram of lignin superimposed with its fine structure (elementary TSC thermograms) obtained by using fractional polarizations

a  $\beta$  relaxation mode characterized by a broad peak with a maximum at  $-90$  °C. This broad relaxation was also resolved into elementary thermograms. The molecular origin of this relaxation mode is the mobility of OH groups of lignin (Roig et al. 2012, 2011b). Data extracted from the series of elementary thermograms permit to plot the variation of the activation enthalpy  $\Delta H$  versus temperature (Fig. 4) in order to compare cellulose and lignin. For cellulose, two different behaviors are underlined. From  $-160$  to  $-90$  °C, the fourteen enthalpy values follow the Starkweather line characteristic of a localized mobility associated with lateral groups of the glycosidic ring. Contrarily, enthalpy values recorded in the temperature ranging from  $-90$  to  $-20$  °C move away progressively from the Starkweather line; this component has been assigned to the delocalized mobility of the  $\text{CH}_2\text{OH}$  lateral groups. For lignin, lateral groups only show a localized mobility.

### Comparison between molecular mobility of cellulose and rosewood

Rosewood was also analyzed by DDS in the low temperature range and compared to cellulose. The variation of  $\tan(\delta)$  versus temperature for cellulose and rosewood is plotted in Fig. 5 at 1 Hz. The relaxation mode of rosewood seems similar to the one of cellulose with a maximum at around  $-120$  °C. The insert in Fig. 5 shows the temperature dependence of the average relaxation time of  $\tan(\delta)$ : In both cases, they follow an Arrhenius law. However, the activation enthalpy value of rosewood is higher than the one of cellulose. Consequently, the molecular mobility of this relaxation is restricted by the matrix surrounding cellulose in rosewood.

In Fig. 6, the normalized depolarization current  $\sigma$  of rosewood recorded by TSC is plotted versus temperature. The complex thermogram reveals a large peak between  $-150$  and  $-60$  °C. The experimental resolution in elementary thermograms highlights two relaxation modes. Indeed, two series of elementary

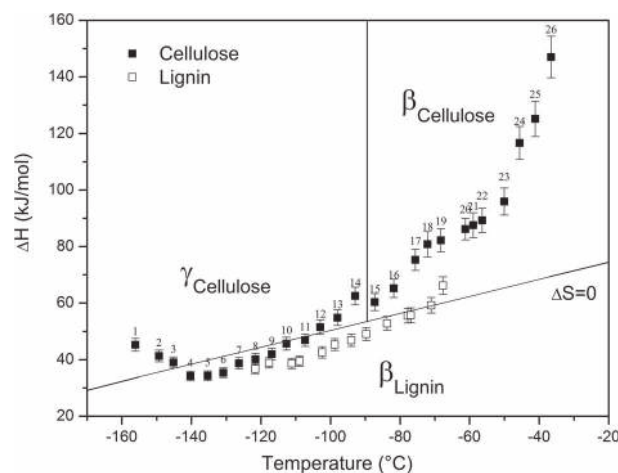


**Fig. 4** Activation enthalpy of the elementary TSC thermograms as a function of temperature for cellulose (black square) and lignin (open square). The Starkweather line  $\Delta S = 0$  is indicated as reference

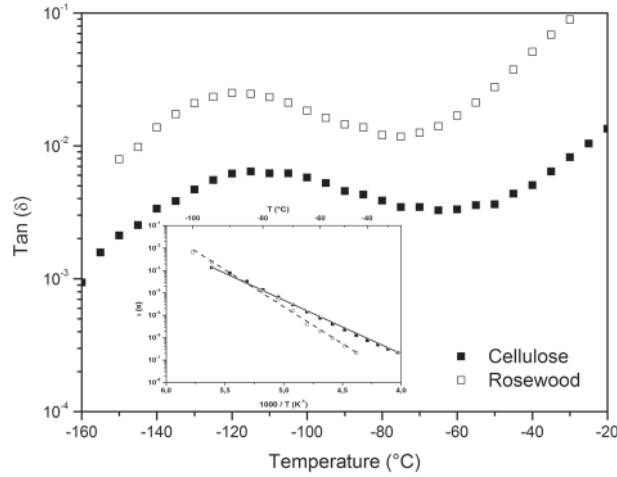


**Fig. 5** Dielectric  $\tan\delta$  versus temperature at the frequency  $F = 1$  Hz of the low-temperature relaxation mode observed by DDS for cellulose (*black square*) and rosewood (*open square*); *inset* Arrhenius diagram of the average relaxation time from  $10^{-1}$  to  $10^{+6}$  isofrequencies

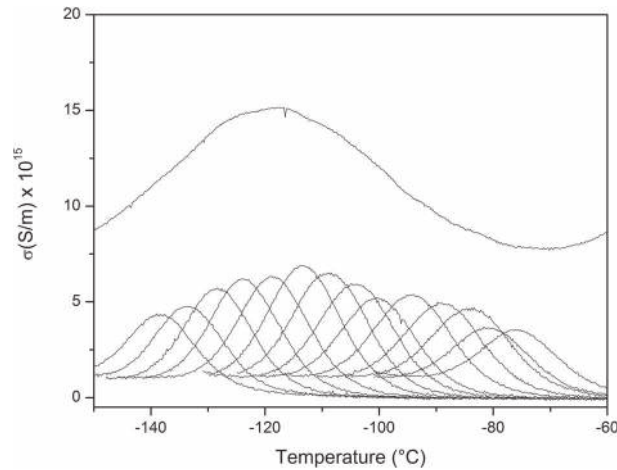


**Fig. 6** Complex TSC thermogram of ebony superimposed with its fine structure (elementary TSC thermograms) obtained by using fractional polarizations

thermograms are observed that reach a maximum at  $-113$  and  $-94$  °C, respectively. The enthalpy diagram of Fig. 7 confirms that rosewood has two relaxation modes. The points between  $-130$  and  $-90$  °C are close to the Starkweather line, contrary to the points after  $-90$  °C, which progressively move away from the Starkweather line. In the order of increasing temperature, the first relaxation mode corresponds to a localized mobility and the second relaxation mode reflects a delocalized mobility. Thanks to the comparison with cellulose in the same temperature range (black squares in Fig. 7), a common molecular origin is attributed

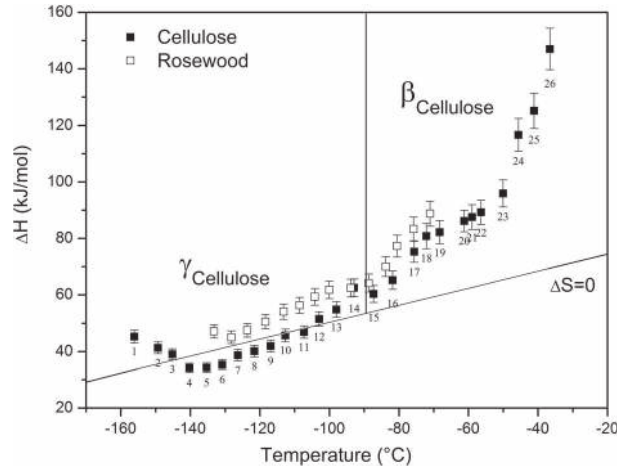


**Fig. 7** Activation enthalpy of the elementary TSC thermograms as a function of temperature for cellulose (*black square*) and rosewood (*open square*). The Starkweather line  $\Delta S = 0$  is indicated as reference

to the relaxations of cellulose and rosewood. In consequence, as Jafarpour et al. (2008) had found in poplar, localized molecular mobility of rosewood is the response of cellulose in plant-based composites. This response is not exactly the same as cellulose *ex situ* because in plant-based composites, cellulose is in a confined state and linked to other constituents of the cell wall with hydrogen bonds. For rosewood as for cellulose, the  $\gamma_{\text{Cellulose}}$  relaxation mode is attributed to molecular mobility of lateral groups of glycosidic rings ( $-\text{OH}$  and  $-\text{CH}_2\text{OH}$ ) and the  $\beta_{\text{Cellulose}}$  relaxation mode is associated with molecular mobility of glycosidic rings around the  $\beta_{1-4}$  glycosidic bonds (Jafarpour et al. 2007, 2009; Einfeldt et al. 2004).

### Comparative dynamic mobility of three different woods

Figures 8 and 9 show the  $\tan(\delta)$  loss factor at 1 Hz plotted versus temperature recorded by two complementary techniques: dynamic mechanical and dynamic dielectric analyses. For rosewood, ebony and varongy, only one relaxation was observed in the temperature range between  $-150$  and  $-20$  °C. This analogy indicates a strong coupling between mechanical and dielectric relaxations. The corresponding average relaxation time was plotted versus temperature in an Arrhenius diagram (Fig. 10). For this complex mode, the values of enthalpy are practically identical for the three species.

Rosewood, ebony and varongy were also studied by TSC in the same temperature range. The normalized depolarization current of the three woods was recorded versus temperature, and the analysis is reported in the enthalpy diagram of Fig. 11. Varongy and ebony exhibit three series of values which determine three relaxation modes, contrary to rosewood which exhibits only two relaxation modes as shown in the preceding section. For varongy and ebony, the three series of enthalpy values are close to the Starkweather line. The molecular mobility is localized. Thanks to the

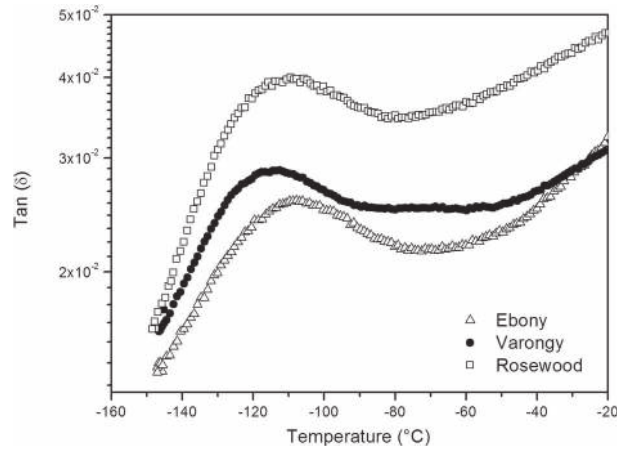


**Fig. 8** Mechanical  $\tan\delta$  versus temperature at the frequency  $F = 1$  Hz for the low-temperature relaxation mode observed by DMA for varongy (filled circle), rosewood (open square) and ebony ( $\Delta$ )

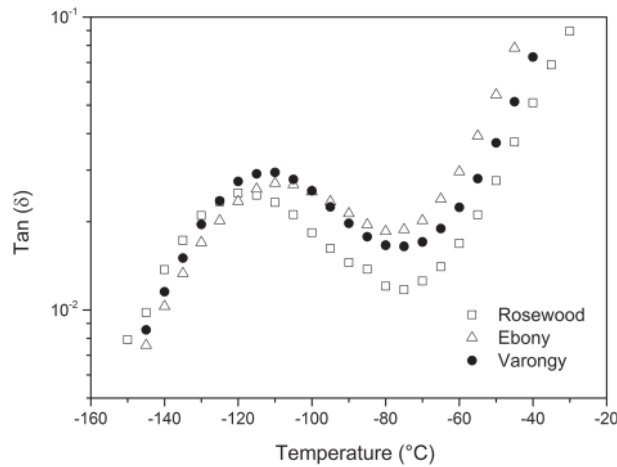


**Fig. 9** Dielectric  $\tan\delta$  versus temperature at the frequency  $F = 1$  Hz for the low-temperature relaxation mode observed by DDS, for varongy (black square), rosewood (open square) and ebony ( $\Delta$ )

comparison with results of extracted cell wall polymers, each relaxation mode can be attributed. For ebony and varongy,  $\gamma_{\text{Cellulose}}$ ,  $\beta_{\text{Lignin}}$  and  $\beta_{\text{Cellulose}}$  are identified. However, except for  $\beta_{\text{Lignin}}$  of ebony all the other enthalpy values of different relaxation modes tend to move away from the Starkweather line. If this tendency is classic for  $\beta_{\text{Cellulose}}$  because for cellulose alone this mobility is delocalized, it is more original for  $\gamma_{\text{Cellulose}}$  of varongy and ebony and  $\beta_{\text{Lignin}}$  of varongy. For each species of wood, the molecular mobility is modified by its specific environment.

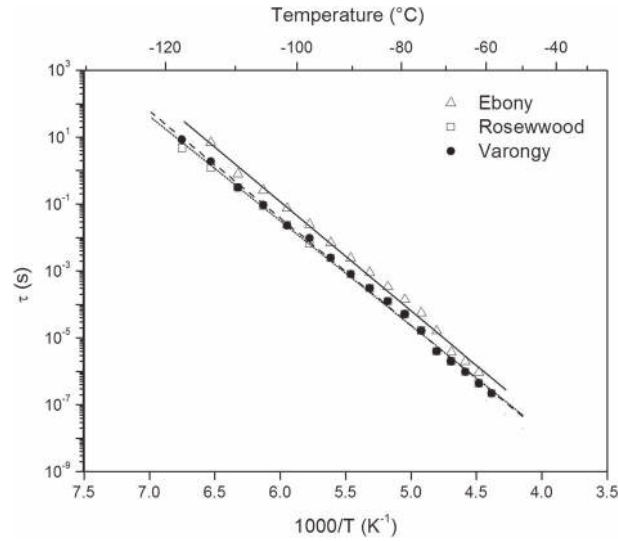


**Fig. 10** Arrhenius diagram of the average relaxation time from  $10^{-1}$  to  $10^{+6}$  isofrequencies, for varongy (filled circle), rosewood (open square) and ebony ( $\Delta$ )

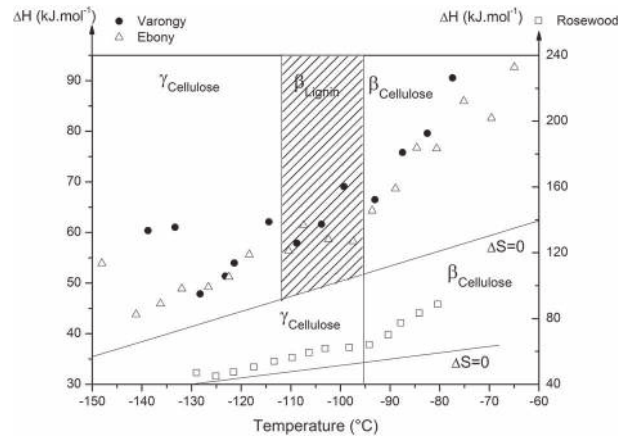


**Fig. 11** Activation enthalpy of the elementary TSC thermograms as a function of temperature, for varongy (filled circle), rosewood (open square) and ebony (open triangle). The Starkweather line  $\Delta S = 0$  is indicated as reference

### Molecular origin of the dynamic response

In order to interpret the molecular mobility in wood, the response of the two main constituents (cellulose and lignin) was used as reference. The evolution of the dynamic responses in the various woods will be discussed.

---

### $\gamma_{\text{Cellulose}}$

This mode is located between  $-150$  and  $-110$  °C with an enthalpy range between 30 and 60 kJ/mol (Figs. 4, 7, 11). All the enthalpy values of the three woods or cellulose ex situ were close to the Starkweather line. Consequently, this relaxation is due to a localized molecular mobility. According to the literature, this mode has been attributed to the molecular mobility of hydroxyl and hydroxymethyl groups of cellulose (Obataya et al. 1996; Saad and Furuhashi 1997; Einfeldt et al. 2000a, b, 2001, 2003; Einfeldt and Kwasniewski 2002; Meissner et al. 2000; Jafarpour et al. 2007, 2009). The size of those mobile units is compatible with the enthalpy and entropy values.

### $\beta_{\text{Lignin}}$

This relaxation is detected between  $-110$  and  $-70$  °C with enthalpy values from 30 to 70 kJ/mol (Figs. 4, 11). Due to its small magnitude, its observation is difficult. It is often masked by  $\gamma_{\text{Cellulose}}$  that is ten times more intense. Only few authors identified the response of lignin in plants. Jafarpour et al. (2008) found two components for the dielectric manifestation of poplar glass transition: one associated with the response of cellulose and the second associated with lignin. Roig et al. (2011b, 2012) associated  $\beta_{\text{Lignin}}$  with the molecular mobility of hydroxyl group of lignin; this assignment sounds consistent with the observed data.

### $\beta_{\text{Cellulose}}$

$\beta_{\text{Cellulose}}$  was defined between  $-90$  and  $-40$  °C with an enthalpy ranging from 60 to 160 kJ/mol (Figs. 4, 7, 11). If the molecular origin of  $\gamma_{\text{Cellulose}}$  mode is clear, the one of  $\beta_{\text{Cellulose}}$  relaxation has been a subject of controversy. Nowadays,  $\beta_{\text{Cellulose}}$  is associated with the molecular mobility of glycosidic rings thanks to  $\beta_{1-4}$  glycosidic bonds (Meissner et al. 2000; Roig et al. 2011a).

## Conclusion

This study focused on the low-temperature molecular mobility of three different wood species. Mechanical and dielectric dynamic thermal analyses, showing complex relaxation modes around 1 Hz, were complemented by a very low-frequency analysis with thermostimulated current that allows to observe the fine structure of the broad relaxation modes of wood.

Low-temperature relaxations of rosewood were assigned to a localized low-temperature relaxation of cellulose. There is no dielectric response of lignin in rosewood. This observation might be related to dispersion of lignin in cellulose. Contrarily, both cellulose and lignin responses were distinguished in ebony and varongy. At the scale of a few nm corresponding to low-temperature relaxations, both cellulose and lignin phases segregate. TSC analyses exhibit the peculiarity of the behavior of lignin and cellulose components in the various sapwood species.

---

## References

- Agoudjil B, Benchabane A, Boudenne A, Ibos L, Fois M (2011) Renewable materials to reduce building heat loss: characterization of date palm wood. *Energy Build* 43:491–497
- Backman AC, Lindberg KAH (2001) Differences in wood material responses for radial and tangential direction as measured by dynamic mechanical thermal analysis. *J Mater Sci* 36:3777–3783
- Badry MD, Yousef MA, Nada AMA (1994) Dielectric characteristics of lignin and some cellulosic materials. *Cellul Chem Technol* 28:605–612
- Cao JZ, Zhao GJ (2001) Dielectric relaxation based on adsorbed water in wood cell wall under non-equilibrium state. 2. *Holzforschung* 55:87–92
- Chilcott TC, Halimanto D, Langrish TAG, Kavanagh JM, Coster HGL (2011) Characterizing moisture content and gradients in *Pinus radiata* soft wood using electrical impedance spectroscopy. *Drying Technol* 29:1–9
- Crine JP (1984) A thermodynamic model for the compensation law and its physical significance for polymers. *J Macromolecul Sci Phys* B23:201–219
- Crine JP (2005) On the interpretation of some electrical aging and relaxation phenomena in solid dielectrics. *IEEE Trans Dielectr Electr Insul* 12:1089–1107
- Daian G, Taube A, Birnboim A, Shramkov Y, Daian M (2005) Measuring the dielectric properties of wood at microwave frequencies. *Wood Sci Technol* 39:215–223
- Daian G, Taube A, Birnboim A, Daian M, Shramkov Y (2006) Modeling the dielectric properties of wood. *Wood Sci Technol* 40:237–246
- Duchow KJ, Gerhardt RA (1996) Dielectric characterization of wood and wood infiltrated with ceramic precursors. *Mater Sci Eng C-Biomim Mater Sens Syst* 4:125–131
- Einfeldt J, Kwasniewski A (2002) Characterization of different types of cellulose by dielectric spectroscopy. *Cellulose* 9:225–238
- Einfeldt J, Kwasniewski A, Meissner D, Gruber E, Henricks R (2000a) Dielectric spectroscopic results and chemical accessibility of sulfite pulps. *Macromol Mater Eng* 283:7–14
- Einfeldt J, Meissner D, Kwasniewski A (2000b) Comparison of the molecular dynamics of celluloses and related polysaccharides in wet and dried states by means of dielectric spectroscopy. *Macromol Chem Phys* 201:1969–1975
- Einfeldt J, Meissner D, Kwasniewski A (2001) Polymerdynamics of cellulose and other polysaccharides in solid state-secondary dielectric relaxation processes. *Prog Polym Sci* 26:1419–1472
- Einfeldt J, Meissner D, Kwasniewski A (2003) Contributions to the molecular origin of the dielectric relaxation processes in polysaccharides—the high temperature range. *J Non-Cryst Solids* 320:40–55
- Einfeldt J, Meissner D, Kwasniewski A (2004) Molecular interpretation of the main relaxations found in dielectric spectra of cellulose—experimental arguments. *Cellulose* 11:137–150
- Havriliak S, Negami S (1966) A complex plane analysis of  $\alpha$ -dispersions in some polymer systems. *J Polym Sci Part C: Polym Symp* 14:99–117
- Hirai N, Hayamura S, Suzuki Y, Miyajima K, Matsuyama S (1992) Piezoelectric relaxation of wood in high-temperature region. *Mokuzai Gakkaishi* 38:820–824
- Hoffman JD, Williams G, Passaglia E (1966) Analysis of  $\alpha$ ,  $\beta$  and  $\gamma$  relaxations in Polychlorotrifluoroethylene and Polyethylene: dielectric and mechanical properties. *J Polym Sci Part C: Polym Symp* 14:173–234
- Hoffmann G, Poliszko S (1996) Temperature-frequency transformation in dielectric thermal analysis (DETA) of wood relaxation properties. *J Appl Polym Sci* 59:269–275
- Jafarpour G, Dantras E, Boudet A, Lacabanne C (2007) Study of dielectric relaxations in cellulose by combined DDS and TSC. *J Non-Cryst Solids* 353:4108–4115
- Jafarpour G, Dantras E, Boudet A, Lacabanne C (2008) Molecular mobility of poplar cell wall polymers studied by dielectric techniques. *J Non-Cryst Solids* 354:3207–3214
- Jafarpour G, Roig F, Dantras E, Boudet A, Lacabanne C (2009) Influence of water on localized and delocalized molecular mobility of cellulose. *J Non-Cryst Solids* 355:1669–1672
- Jonoobi M, Oladi R, Davoudpour Y, Oksman K, Dufresne A, Hamzeh Y, Davoodi R (2015) Different preparation methods and properties of nanostructured cellulose from various natural resources: a review. *Cellulose* 22:935–969
- Kabir MF, Khalid KB, Daud WM, Aziz SHA (1997) Dielectric properties of rubber wood at microwave frequencies measured with an open-ended coaxial line. *Wood Fiber Sci* 29:319–324



- 
- Kabir MF, Daud WM, Khalid K, Sidek HAA (1998a) Dielectric and ultrasonic properties of rubber wood. Effect of moisture content, grain direction and frequency. *Holz Roh- Werkst* 56:223–227
- Kabir MF, Daud WM, Khalid K, Sidek HAA (1998b) Effect of moisture content and grain direction on the dielectric properties of rubber wood at low frequencies. *Holzforschung* 52:546–552
- Kabir MF, Daud WM, Khalid KB, Sidek AHA (2000) Equivalent circuit modeling of the dielectric properties of rubber wood at low frequency. *Wood Fiber Sci* 32:450–457
- Khalid KB, Kabir MF, Daud WM, Sidek HAA (1999) Multi-component mixture modeling for the dielectric properties of rubber wood at microwave frequencies. *Holzforschung* 53:662–668
- Koubaa A, Perre P, Hutcheon RM, Lessard J (2008) Complex dielectric properties of the sapwood of aspen, white birch, yellow birch, and sugar maple. *Drying Technol* 26:568–578
- Luiz de Paula E, Mano V, Pereira FV (2011) Influence of cellulose nanowhiskers on the hydrolytic degradation behavior of poly(D, L-lactide). *Polym Degrad Stab* 96:1631–1638
- Maeda H, Fukada E (1987) Effect of bound water on piezoelectric, dielectric, and elastic properties of wood. *J Appl Polym Sci* 33:1187–1198
- Makoviny I (2000) Dielectric and electromagnetic characteristics of beech wood. *Drevarsky Vyskum* 45:23–34
- Marianoa M, El Kissic N, Dufresne A (2016) Cellulose nanocrystal reinforced oxidized natural rubber nanocomposites. *Carbohydr Polym* 137:174–183
- Meissner D, Einfeldt J, Kwasniewski A (2000) Contributions to the molecular origin of the dielectric relaxation processes in polysaccharides—the low temperature range. *J Non-Cryst Solids* 275:199–209
- Mobarak F, Mounir M, Mohsen F, Ali AFH (1999) Studies on the electrical properties of agricultural residues paper. I. Electrical properties of cotton stalks and wood papers. *Cellul Chem Technol* 33:321–331
- Mounier M, Mohsen F, Ali AFH, Mobarak F (1999) Studies on the electrical properties of agricultural residue papers II. Electrical properties of rice straw paper and its blends with cotton stalks and wood. *Cellul Chem Technol* 33:513–525
- Nakano T (2004) Mechanical relaxation and physical properties of wood. *Mokuzai Gakkaishi* 50:203–213
- Nakano T (2005) Effects of quenching on relaxation properties of wet wood. *J Wood Sci* 51:112–117
- Obataya E, Yokoyama M, Norimoto M (1996) Mechanical and dielectric relaxations of wood in a low temperature range. I. Relaxations due to methylol groups and adsorbed water. *Mokuzai Gakkaishi* 42:243–249
- Obataya E, Norimoto M, Tomita B (2001) Mechanical relaxation processes of wood in the low-temperature range. *J Appl Polym Sci* 81:3338–3347
- Ramasamy S, Moghtaderi B (2010) Dielectric properties of typical Australian wood-based biomass materials at microwave frequency. *Energy Fuels* 24:4534–4548
- Roig F, Dantras E, Dandurand J, Lacabanne C (2011a) Influence of hydrogen bonds on glass transition and dielectric relaxations of cellulose. *J Phys D-Appl Phys* 44:045403
- Roig F, Dantras E, Grima-Pettenati J, Lacabanne C (2011b) Thermo Stimulated Currents a Method to Identify Gene Mutation in Arabidopsis Thaliana. 2011–14th International Symposium on Electrets (ISE), pp 175–176
- Roig F, Dantras E, Grima-Pettenati J, Lacabanne C (2012) Analysis of gene mutation in plant cell wall by dielectric relaxation. *J Phys D Appl Phys* 45:295402
- Romanov AN (2006) The effect of volume humidity and the phase composition of water on the dielectric properties of wood at microwave frequencies. *J Commun Technol Electron* 51:435–439
- Saad GR, Furuhashi K (1997) Effect of substituents on dielectric beta-relaxation in cellulose. *Polym Int* 42:356–362
- Saad GR, Sakamoto M, Furuhashi K (1996) Dielectric study of  $\beta$ -relaxation in some cellulosic substances. *Polym Int* 41:293–299
- Sahin H, Ay N (2004) Dielectric properties of hardwood species at microwave frequencies. *J Wood Sci* 50:375–380
- Starkweather HW (1981) Simple and complex relaxations. *Macromolecules* 14:1277–1281
- Starkweather HW (1990) Distribution of activation enthalpies in viscoelastic relaxations. *Macromolecules* 23:328–332
- Starkweather HW, Avakian P (1989) Beta-relaxations in phenylene polymers. *Macromolecules* 22:4060–4062
- Sugimoto H, Norimoto M (2005) Dielectric relaxation due to the heterogeneous structure of wood charcoal. *J Wood Sci* 51:554–558

- 
- Sugimoto H, Takazawa R, Norimoto M (2005) Dielectric relaxation due to heterogeneous structure in moist wood. *J Wood Sci* 51:549–553
- Sugimoto H, Miki T, Kanayama K, Norimoto M (2008a) Dielectric relaxation of water adsorbed on cellulose. *J Non-Cryst Solids* 354:3220–3224
- Sugimoto H, Miki T, Nishida M, Kanayama K (2008b) Ivth International Conference on Times of Polymers, ed D D A G L Acierno pp 138–140
- Teyssedre G, Lacabanne C (1995) Some considerations about the analysis of thermostimulated depolarization peaks. *J Phys D-Appl Phys* 28:1478–1487
- Tomppo L, Tiitta M, Laakso T, Harju A, Venalainen M, Lappalainen R (2009) Dielectric spectroscopy of Scots pine. *Wood Sci Technol* 43:653–667
- Wang Y, Minato K, Iida I (2008) Mechanical properties of wood in an unstable state due to temperature changes, and analysis of the relevant mechanism VI: dielectric relaxation of quenched wood. *J Wood Sci* 54:16–21
- Yelon A, Movaghar B, Branz HM (1992) Origin and consequences of the compensation (meyer-neldel) law. *Phys Rev B* 46:12244–12250
- Yokoyama M, Kanayama K, Furuta Y, Norimoto M (2000a) Mechanical and dielectric relaxations of wood in a low temperature range III. Application of sech law to dielectric properties due to adsorbed water. *Mokuzai Gakkaishi* 46:173–180
- Yokoyama M, Ohmae K, Kanayama K, Furuta Y, Norimoto M (2000b) Mechanical and dielectric relaxations of wood in a low temperature range IV. Dielectric properties of adsorbed water at high moisture contents. *Mokuzai Gakkaishi* 46:523–530